11th International Conference on Marine Technology
MARTEC 2018

MODELLING ON NUMERICAL WAVE TANK FOR APPLICATION OF OWC SIMULATION

A. M. A. Rahim[a], O. B. Yaakob[a,b], C. L. Siow[a,b]

[a] School of Mechanical Engineering,
Faculty of Engineering,
Universiti Teknologi Malaysia,
81310 UTM Skudai, Malaysia

[b] Marine Technology Center,
Universiti Teknologi Malaysia,
81310 UTM Skudai, Malaysia

ABSTRACT

This paper presents a development of numerical wave tank uses to develop and simulate the phenomena of OWC experiment by domain transfer method from 2D experimental data to 3D effect domain by expanding the wall. The CFD will be validated with experimental data from published paper and the performance of the simulation setup will be evaluated by using Nash and Sutcliffe (NSE) model efficiency coefficient and the mean square error (MSE). The OWC experiment phenomena were simulated using Flow 3D CFD Software and results are presented in the form of maximum air velocity and maximum air pressure. The validation model performance result was 0.993 for NSE and the MSE was 0.157. The optimum width ratio of the distance between the wall and the width of OWC obtain from this study was less than 0.2.

Keywords: *Wave Energy, Oscillating Water Column, CFD Validation, FLOW-3D*

1.0 INTRODUCTION

In the developing country, the energy resources are the important factor in economic growth. Most of the energy resources come from non-renewable resources which can also pollute the environment. The alternative to this problem is using renewable energy.. One form of renewable energy is ocean energy which is predictable and largely available in Malaysia. There are various studies in the development of the devices for extracting the ocean energy in Malaysian sea[1]. One of the most reliable devices are Oscillating Water Column (OWC) due to no moving part interact with sea water. The OWC generates the electricity by converting the energy of fluctuation air produced by the reciprocating motion of water inside the chamber through an air turbine attached to a generator. Studies suggest that significant wave height and a significant period are among the most important factors influencing the development of OWC parameters[2]. This paper presents a study to develop an OWC for the remote island of Pulau Tinggi in Johor. . The wave data for this location are

*Corresponding author: amustaqim23@live.utm.my

referred to latest wave data statistic using satellite altimeter[3]. The significant wave height for this location is 0.75m and the significant period is 5.5s[3].

Currently, most of OWC development focus on integration OWC caisson with breakwater but no study has been conducted to develop floating OWC in Malaysia sea condition. Many methods have been used to improve wave power conversion. For example Shimosako et al. (2016) introduced a projecting wall in front of the OWC which increased the efficiency by 10% compared with the standard OWC[4]. The application of projecting wall began in 1985 with studies on the effect of placing projecting sidewalls in front of the column done by [5]. Furthermore, study the relationship between the effect of the wall in flume tank experiment and the efficiency of OWC done by [6]who has shown a strong evidence that wall effect will overestimate the efficiency value of OWC.

Results from earlier studies demonstrate a strong and consistent association between projecting wall/side wall and the increase in power absorption. In this study, the U-Channel will be added in front of the OWC floating fix-type. U-Channel named after the shape of additional structure in form of U (see Figure 1). The simulation software Flow-3D and the modeling development was carried out using Autodesk Inventor 2017 student edition. Numerical modelling by CFD method was ideal method to develop the OWC due to lower cost than experiment [7]and the numerical wave tank (NWT) was used to develop OWC without any distraction or wave reflection by the wall. The NWT was developed by domain transfers from 2D experimental data to 3D effect domain to avoid overestimation on 2D NWT. The advantages of 3D NWT is capable to demonstrate a good prediction interaction between free surface elevation of the water, the variation of the air pressure, and the dynamic motion of the air flow[8]. The simulation will be validated with published results and and the simulation setup can be used for further OWC development.

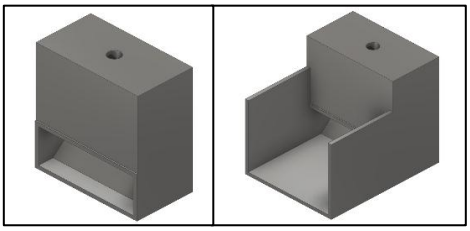

Figure 1: Initial model in the left-side picture and additional U-Channel in front of an initial model on the right-side picture.

2.0 OWC Performance

In this study, the OWC performance is indicated by efficiency [$\boldsymbol{\eta_{owc}}$] in Equation 1 [9] by dividing the power generated by air at OWC's orifice (P_{air}) with the power of incident wave (P_{inc}) measured at wave probe. The power generated by air is obtained by measuring two parameters from the simulation results; the mean air volume flow rate [q(t)] produced by the OWC's orifice in m^3/s and the instantaneous air pressure[p(t)] at the OWC's orifice in Pascal.

$$\boldsymbol{\eta_{owc} = \frac{P_{air}}{P_{inc}} \times 100\%} \quad \textbf{(1)}$$

The efficiency is obtained by The power produced by air in Equation 2 is the energy produced by air at OWC's orifice (E_{air}) divided by wave period (T)[9].

$$\boldsymbol{Power\ produce\ by\ air,\ P_{air} = \frac{E_{air}}{T}} \quad \textbf{(2)}$$

The energy of air in Equation 3 can be obtained by measuring the instantaneous air pressure [*p(t)*] using probe in Pascal (*Pa*) unit and the air velocity was measured in meter per second to get the discharge rate [*q(t)*] by multiply the air velocity and the area of orifice[9].

$$\textbf{Energy produce by air, } E_{air} = \int_0^T p(t)q(t)dt \quad \textbf{(3)}$$

The power of incident wave (P_{inc}) per unit width (W/m) in Equation 4 was calculated by multiplying the wave energy (E) and wave group celerity (C_g)[9].

$$P_{inc} = EC_g(Wm^{-1}) \quad \textbf{(4)}$$

The wave energy in Equation 5 consists of the density of water (ρ) multiplies by gravitational forces (g) and amplitude of incident wave (a_0)[9].

$$\textbf{Wave Energy, } E = \frac{1}{2}\rho g a_0{}^2 \quad \textbf{(5)}$$

The wave group velocity (C_g) in Equation 6 considers the average water depth (h), the wave velocity (c) and the wave number (k)[9].

$$C_g = \frac{d\omega}{dk} = \frac{c}{2}\left[1 + \frac{2kh}{\sin 2\,kh}\right] \quad \textbf{(6)}$$

3.0 CFD Validation and Domain Transfer Method

This study uses the commercial software Flow-3D 11.0.4 version as the simulation tool. Flow-3D uses the Volume-of-Fluid (VOF) method to model free surface [10]. The VOF method was used to track the surface as a sharp interface moving through a computational grid and applying boundary condition at the surface. Hence in the VOF method, the validation is the crucial step in proving the simulation setup are closely reflect the actual event. Most of researcher use mathematical solution to determine the effectiveness of the simulation setup[11] and for this study, Mean Square Error (MSE) and Nash-Sutcliffe coefficient of efficiencies (NSE) was used and the further explanation on section 3.3.

The validation of the simulation done by comparing the result of the simulation with the experiment carried out by Kuo et al. 2017. This experiment was done in flume tank and the OWC devices are the basic rectangular shape (see Figure 2). The dimensions given are for the inner side of OWC. The opening mouth of the OWC is 0.19m x 0.5m while the diameter of the orifice is 0.1m.

The instrument and configuration of the experiment shown in Figure 3. The water level for the experiment was 0.25m and the initial fluid elevation in the simulation set to 0.25m. The wall of the flume tank was height 0.6m and the distance between wavemaker and the end of OWC was 15.85m.

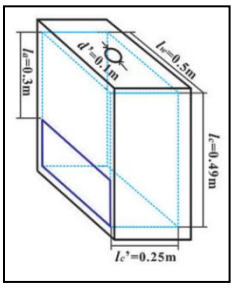

Figure 2: The OWC uses in experiment by Kuo et al. 2017.[9]

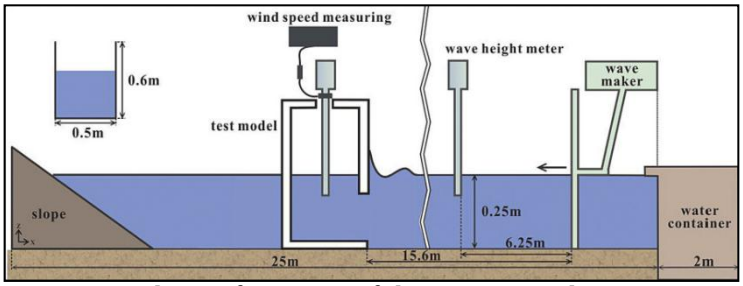

Figure 3: The configuration of the experiment by Kuo et al. 2017.[9]

This simulation uses the two-fluid method due to interface between air and water. In this model, fluid 1 was set to water and the value of the fluid fraction for fluid 1 was set to 1. Fluid 2 was set to air and the value of the fluid fraction was set to 0. This fraction value describes the mixture between this fluid. Figure 4 show clearly the separation of air and water at the water level along simulation time.

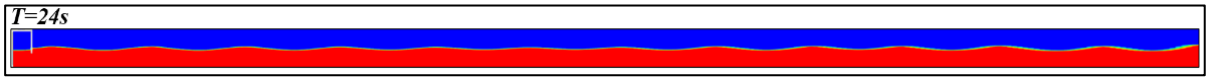

Figure 4: Fluid fraction along simulation time.

3.1. Boundary Condition

The simulation tool Flow-3D uses a Cartesians system (x,y,z) to locate each coordinate in the simulation. The meshing configuration was defined by; 1) Z_{min} and Z_{max} for the height of bottom of domain till top domain which is 0.51m for z-axis, 2) X_{min} and X_{max} for the length between front domain till back of domain which is 15.89m for x-axis and 3) Y_{min} and Y_{max} are for the width of left of flume tank till right side of flume tank which is 0.5m. for y-axis.

Most researchers uses uniform grid technique for the meshing [9], [11], but this technique will consume more simulation time due to the high number of meshing cells. In this study, mesh plane method (see Figures 5 & 6) was used to define a meshing cell size to reduce the meshing cell and simulation time. The meshing cell size was refined at the water surface and the height for this plane was made equal to the wave height due to this section are an interaction between air and water. The domain size was cut off from the back of OWC till the end of flume tank due to no activity behind of OWC to simulate.

To reflect the simulation setup with the real condition in an experiment, boundary conditions were set up based on the configuration of the experiment. Figure 5 shows the top boundary which is Z_{max} boundary was set to specific pressure of 101325 Pa which is the same as the atmospheric pressure in the experiment. The floor, the left side, the right side and the last section of the domain which is Z_{min}, Y_{min}, Y_{max} and X_{min} was set to wall boundary condition. In front of domain which is X_{max} boundary set to wave boundary control to generate the wave same as wave maker in Figure 3.

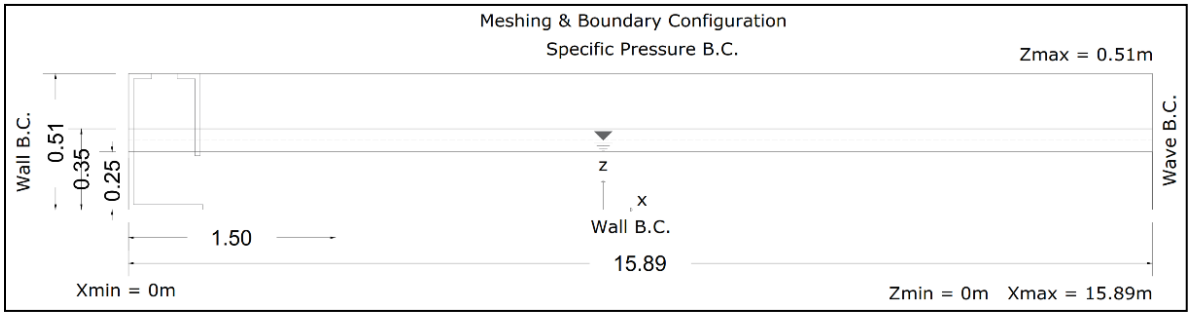

Figure 5: Meshing and boundary condition.

The probe placement was located according to the experiment configuration in Figure 3. The entry of wave characteristics in the simulation must be calibrated at the wave probe in simulation with the value of wave amplitude and period in the experiment. The wave calibration in simulation is to obtain the same wave characteristic with experiment to avoid a large error in result. Table 1 shows the entry of calibrated wave amplitude and period value in the simulation.

Wave Amplitude Experiment (m)	Wave Amplitude Simulation Entry (m)	Wave Period Experiment (s)	Wave Period Simulation Entry (s)
0.03	0.042	1	1.007
0.03	0.038	1.2	1.22
0.03	0.037	1.4	1.41
0.03	0.0301	1.6	1.61

Table 1: Entry of calibrate wave amplitude and period value in simulation.

3.2. Grid Independence Study

The total number of meshing cells depends on meshing size. Finer mesh cell size means more mesh cell numbers and more resources are required to run the simulation. Grid independence study was carried out to find an optimum cell size for the simulation. In this simulation, mesh plane method was used to define the meshing of a domain (see Figure 6).

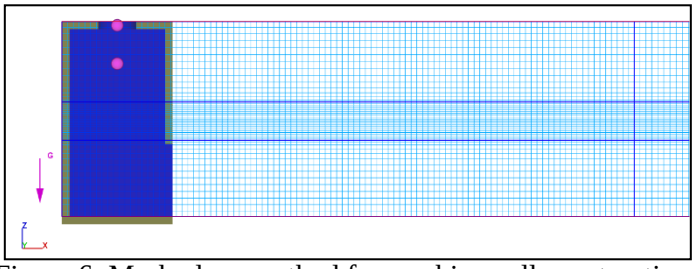

Figure 6: Mesh plane method for meshing cell construction.

The grid independence study starts with the coarse cell size with 0.49 million cell count and up to 1.36 million. The grid dependence study covers all wave characteristic in the experiment to evaluate the pattern of the validation graph.

3.3. Performance evaluation criteria

The performance of the simulation setup was evaluated using Mean Square Error (MSE) and Nash-Sutcliffe coefficient of efficiencies (NSE) which are widely used by the researchers to evaluate the performance of the simulation setup[11]. The MSE was used to show the accuracy of the simulation while the NSE was used to find a goodness of fit between the observed data comparison with benchmark data[11]. The MSE and NSE calculations are shown in Equation 7 and Equation 8.

$$\boldsymbol{Mean\ Square\ Error, MSE} = \sum_{i=1}^{n}(E_i - N_i)^2 \quad \textbf{(7)}$$

$$\boldsymbol{Nash\ and\ Sutcliffe,\ NSE} = \left[1 - \frac{\sum_{i=1}^{n}(E_i - N_i)^2}{\sum_{i=1}^{n}(E_i - E_a)^2}\right] \quad \textbf{(8)}$$

The total numbers of observation data, n in this study was four bases on four wavelength ratios been validated. Results of maximum air velocity, E_i from the experiment were obtained from experimental data done by Kuo et al. 2017[9] shown on Figure 6 and compared with numerical data for maximum air velocity, N_i acquired from the first wave till wave number ten. The average of mean air velocity from experiment model, E_a was the sum of the average of air velocity for all wavelength ratio.

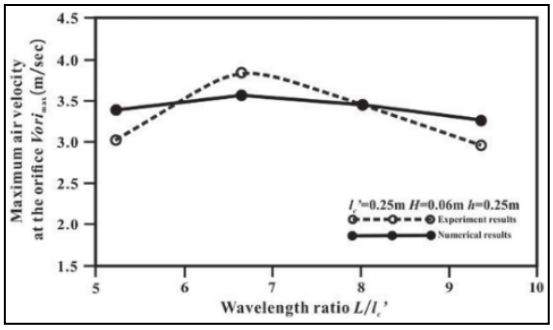

Figure 6: Result experimental data from Kuo et al. 2017[9].

3.4. Domain Transfer

Domain transfer is the method translation the 3D domain from validated 2D domain with flume tank experiment. In this study is to develop an OWC with additional structure in front of OWC. To avoid unwanted interaction reflective wave between OWC and side wall, the wall will be expanded until the optimum distance between the wall and passive slope was added at the end of the domain[12]. The domain from validation will expand in 3-axis (x,y,z)(see Figure 7). The meshing for validation will remain the same, only the rest of expansion will investigate.

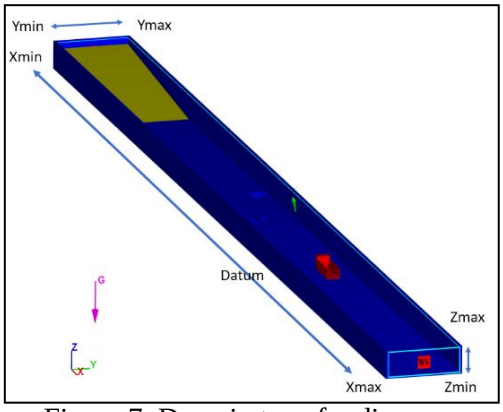

Figure 7: Domain transfer diagram.

The result from the new domain is acceptable because of the validity has been shown based on the flume tank experiment and that section of meshing remain the same[6]. The OWC will be placed at the datum of the domain (x=0, y=0, and z=0). The distance of datum to X_{min} will be based on four-time wavelengths to allow time for wave to pass the OWC and reflect from the OWC The time requirement is enough for ten wave passes through OWC. Meanwhile, the distance from X_{max} to datum remain the same as validation distance.

The height of Z_{max} was determined by the position of the highest height of OWC devices in domain and the height of Z_{min} from the water level was based on the lowest water depth of 3m at Pulau Tinggi [13]. The height of Z_{max} was proven in Z_{max} study (see Figure 9) shown that the height of Z_{max} did not much affect the output of OWC. Hence that, the minimum of Z_{max} was selected to reduce the meshing cell count.

The distance between Y_{min} and Y_{max} determine by the result of wall effect study (WES). Minimum is 0.5m same distance with validation domain in the y-axis and the list of wall effect study in Table 2 below. The wall effect study was done with one wave characteristic only which is wave height, H=0.06m and period, T=1s.

Table 2: Wall effect study and description.

Study	Wall Distance (m)	Study	Wall Distance (m)
WES1	0.5	WES8	2.25
WES2	0.75	WES9	2.5
WES3	1	WES10	2.75
WES4	1.25	WES11	3
WES5	1.5	WES12	3.25
WES6	1.75	WES13	3.5
WES7	2		

4.0 Result and Discussion

The validation of the simulation begins with the turbulence model study since the selection of the right model will optimize the accuracy of the result and the simulation time. Besides that, the height of Z_{max} was also taken into consideration to investigate the influence of the top boundary and the air flow out from OWC. To standardize the variable, both studies used the same wave characteristic with wall effect study. Turbulence mode study showed that k-epsilon is the most suitable for the OWC cases (refer to Figure 8). The Renormalized Group (RNG) and k-ω are less accurate compared with k-epsilon.

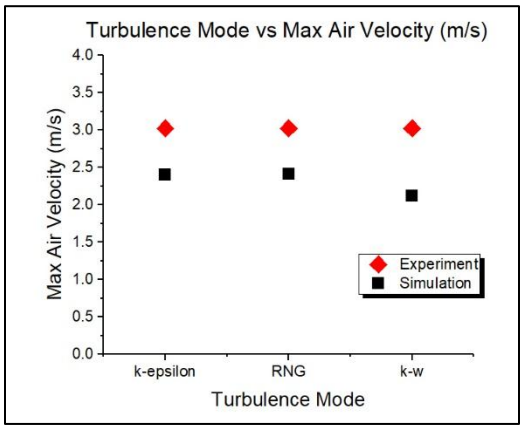

Figure 8: Result turbulence mode study

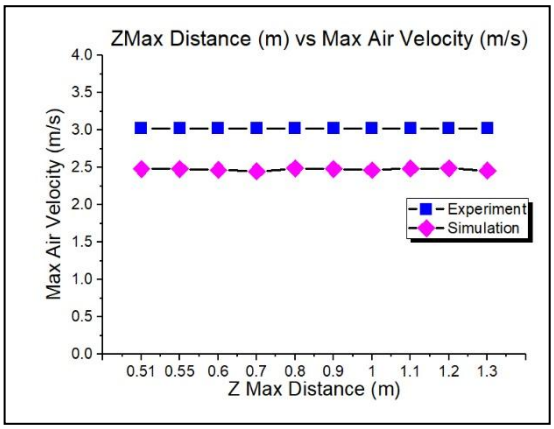

Figure 9: Result for Zmax study.

The k-epsilon turbulence model was selected due to its higher accuracy when compared to the other models as well as its fast fastest simulation time due to its less complex equation. The domain of simulation created exactly same size with experiment flume tank except to the height of Z_{max} due to no limit for uppermost space.

The Zmax study starts from the uppermost OWC up to 1.3m to investigate the optimum height between uppermost OWC and top boundary. The results in Figure 9 show that the height of top boundary and uppermost OWC does not influence in OWC output result. Hence that, the shortest was selected for the height of top boundary to reduce the number of meshing cell.

The k-epsilon turbulence model and 0.51m height for Zmax were used in grid independence study. Grid independence study showed that the 0.63 million meshing cell count is the closest result with experiment (refer Figure 10). The 0.63 million meshing cells shown lower in mean square error compare with another meshing cell configuration and the Nash-Sutcliffe coefficient of efficiencies shown that simulation setup with 0.63 million meshing cells has a good efficiency. The NSE result reflects the outcome of the result from this configuration setup was good as the real condition on the experiment.

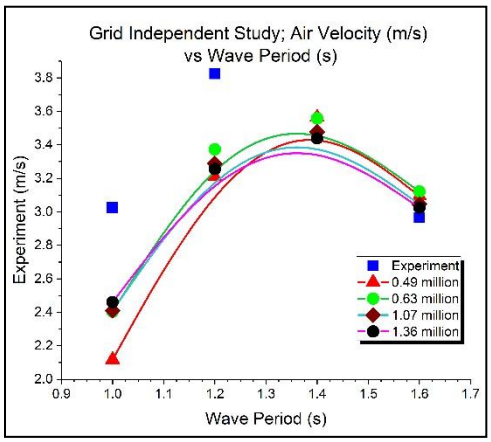

Figure 10: Grid independence study result

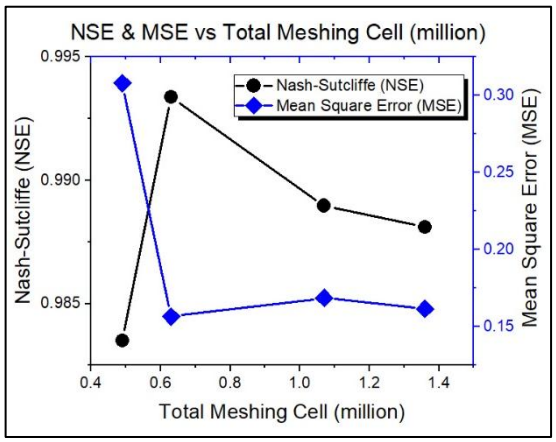

Figure 11: NSE & MSE result

The next step is to study the influence of wall effect on the OWC output. Figure 12 shows the mean air velocity produces at the orifice and the graph start to constant when the wall exceeds 3.25m when the ratio between the width of OWC and the distance of wall is less than 0.2. The effect of the wall also can affect the incoming wave due to reflective wave interaction between the wall and OWC (refer Figure 13). Figure 13 shows wave number from 10^{th} to 17^{th} and the incident wave start to disturb from 10^{th} wave on WES1 while the WES13 shown a consistent wave with no disturbance from the reflective wave.

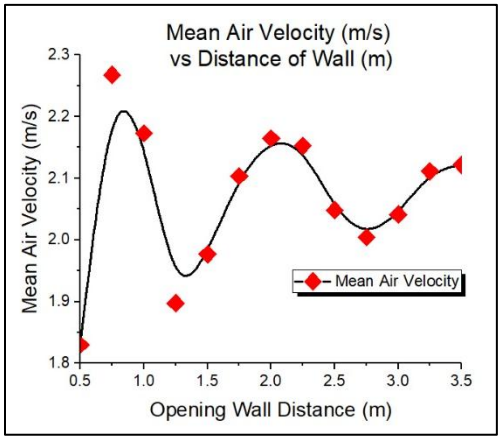

Figure 12: Mean Air Velocity (m/s) Vs Distance of Wall (m)

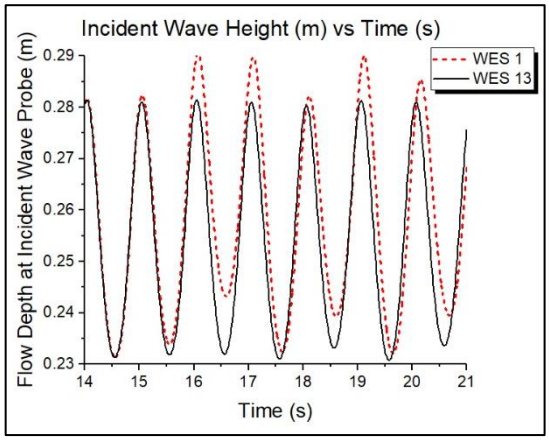

Figure 13: Incident Wave Height (m) Vs Time (s)

5.0 Conclusion

In this study, a numerical wave tank with two fluid VOF technique was established to generate the propagating waves and well validated with flume tank experiment. The comparison between the wall effect and no wall effect were also sufficiently discussed.

It was found that the k-epsilon turbulence model was the most suitable turbulence model to be applied in numerical analysis to develop the OWC. The simulation time also can be reduced by determining the optimum distance between the top boundary and bottom and the use of the mesh plane method in defining computational grid sizing. Finally, the validation from experiment performs a good result to be used for the next stage in the development of OWC.

ACKNOWLEDGEMENT

The author would like to thank Universiti Teknologi Malaysia (UTM) and the Ministry of Higher Education (MOHE) for funding this project under Development Of Combined Ocean Renewable Energy System Prototype (CORES) grant (R.J130000.7824.4L651).

REFERENCE

1. O. Yaakob, T. M. A. Tengku Ab Rashid, and M. A. Abdul Mukti, "Prospects for ocean energy in Malaysia," *... Conf. Energy ...*, vol. 2006, no. Icee, pp. 1–7, 2006.
2. H. Osawa and T. Miyazaki, "Technical manual for oscillating water column type wave power device," *Proc. Fifteenth Int. Offshore Polar Eng. Conf. Seouk, Korea*, vol. 2005, pp. 549–556, 2005.
3. O. Yaakob, F. E. Hashim, K. Mohd Omar, A. H. Md Din, and K. K. Koh, "Satellite-based wave data and wave energy resource assessment for South China Sea," *Renew. Energy*, vol. 88, no. January 2016, pp. 359–371, 2016.
4. K. Shimosako *et al.*, "Model Experiment and Field Test of PW-OWC Type Wave Power Extracting Breakwater," *Coast. Eng.*, pp. 1–10, 2016.
5. O. Malmo and A. Reitan, "Wave-power absorption by an oscillating water column in a channel," *J. Fluid Mech.*, vol. 158, no. September, pp. 153–175, 1985.
6. A. Elhanafi, G. Macfarlane, A. Fleming, and Z. Leong, "Investigations on 3D effects and correlation between wave height and lip submergence of an offshore stationary OWC wave energy converter," *Appl. Ocean Res.*, vol. 64, pp. 203–216, 2017.
7. I. López, B. Pereiras, F. Castro, and G. Iglesias, "Optimisation of turbine-induced damping for an OWC wave energy converter using a RANS-VOF numerical model," *Appl. Energy*, vol. 127, pp. 105–114, 2014.
8. Z. Liu, B.-S. Hyun, and K.-Y. Hong, "Application of numerical wave tank to OWC air chamber for wave energy conversion," vol. 8, pp. 350–356, 2008.
9. Y. S. Kuo, C. Y. Chung, S. C. Hsiao, and Y. K. Wang, "Hydrodynamic characteristics of Oscillating Water Column caisson breakwaters," *Renew. Energy*, vol. 103, pp. 439–447, 2017.
10. Flow Science Inc, *Flow-3D User's Manuals*. Santa Fe, N.M., USA, 2014.
11. F. Mahnamfar and A. Altunkaynak, "Comparison of numerical and experimental analyses for optimizing the geometry of OWC systems," *Ocean Eng.*, vol. 130, no. November 2015, pp. 10–24, 2017.
12. M. A. Mustapa, "Wave Energy Converter - Breakwater System for Wave Energy Shorelines," Universiti Teknologi Malaysia, 2016.
13. S. Y. Gan *et al.*, "Comparison of day and night mysid assemblages in a seagrass bed by using emergence traps , with key to species occurring at Pulau Tinggi , Malaysia," *Coast. Mar. Sci.*, vol. 34, no. 1, pp. 74–81, 2010.